# The quasi 5-day signal in the mesospheric water vapor concentration at high latitudes in 2003-a comparison between observations at ALOMAR and calculations

G. R. Sonnemann,[1,2] P. Hartogh,[2] M. Grygalashvyly,[1] Song Li,[2] and U. Berger[1]

Received 24 April 2007; revised 8 October 2007; accepted 28 November 2007; published 19 February 2008.

[1] A quasi 5-day signature in different middle atmospheric parameters such as the horizontal wind, the temperature, the pressure, the occurrence rate of Polar Mesospheric Summer Echoes (PMSEs) and Noctilucent Clouds (NLCs) or the ozone concentration has been found during the last decades since the 1970s. These effects were interpreted in terms of the impact of a 5-day planetary normal mode (1,1) of Rossby waves. In the mesosphere the quasi 5-day variation is predominantly a summer phenomenon occurring in high and middle latitudes. Water vapor measurements were carried out by means of the microwave technique in high latitudes at ALOMAR (69.29°N, 16.03°E), Norway, for the year 2003. The observations revealed a clear signature of a quasi 5-day variation. Using our real-date Leibniz-Institute Middle Atmosphere (LIMA) model of the Institute of Atmospheric Physics in Kühlungsborn, Germany, in a case study for the same period we found a very clear quasi 5-day signal in the distribution of the minor constituents and particularly in the water vapor mixing ratio in middle to high northern latitudes in the late spring and summer season. A similar finding is valid for the southern hemisphere half a year later. The variations of the minor constituents are triggered by the wind system resulting from the dynamical part of the model. The calculations satisfactorily reproduce the observed water vapor concentrations. In particular, the annual variation including intraannual variations is reflected by the model. We discuss the findings in terms of dynamics and chemistry.

**Citation:** Sonnemann, G. R., P. Hartogh, M. Grygalashvyly, S. Li, and U. Berger (2008), The quasi 5-day signal in the mesospheric water vapor concentration at high latitudes in 2003-a comparison between observations at ALOMAR and calculations, *J. Geophys. Res.*, *113*, D04101, doi:10.1029/2007JD008875.

## 1. Introduction

[2] In addition to the quasi 2-day and 16-day waves, the quasi 5-day wave is one of the most prominent oscillation in the atmosphere. The detection of the 5-day wave, which is really a period between 5 and 7 days and is thus called the quasi 5-day wave, has a long history. Westward-traveling planetary scale waves of different periods have been observed since the 1950s [see *Madden*, 1978, 1979]. *Wallace and Chang* [1969] found hints of a 5-day wave by analyzing large-scale disturbances in the tropical lower troposphere. In 1972 Madden and Julian reported the existence of a 5-day westward moving pressure wave in the troposphere (sea level pressure). A first indication of a stratospheric 5-day wave was given by *Rodgers* [1976] using satellite observation of temperature and later on by *Hirota and Hirooka* [1984] and *Venne* [1985, 1989] for geopotential height. An indication that the 5-day wave comprises nearly all atmospheric layers was found by *Fraser and Thorpe* [1976] and *Fraser* [1977], who reported a 5-day signal in the plasma of the D-region. Hints at a mesospheric 5-day wave were found in radar data in Arecibo [*Hirota et al.*, 1983], however, in low latitudes at 18°N. In 1990 Rosenlof and Thomas derived a 5-day wave from ozone data measured by the Solar Mesosphere Explorer (SME) satellite in high southern latitudes between 50 and 80 km near the December solstice. *Wu et al.* [1994] detected a 5-day planetary wave in the wind data measured by the High Resolution Doppler Imager (HRDI) on the Upper Atmospheric Research Satellite (UARS) between 50 and 110 km. They investigated the phenomenon on a global scale. Different additional groups found a 5-day wind oscillation in the mesosphere [e.g., *Massebeuf et al.*, 1981; *Manson et al.*, 1982; *Vincent*, 1984; *Williams and Avery*, 1992; *Riggin et al.*, 2006]. *Liu et al.* [2004] discussed a 6.5-day wave on the basis of TIME-GCM simulations a period ranging between 5 and 7 days. The period can change by the Doppler shift due to atmospheric winds by less than a half day. Also, *Meyer and Forbes* [1997] showed that the actual wave period, at least for the strong wave event in 1993, was 6 to 7 days.

[1]Leibniz-Institute of Atmospheric Physics at the University Rostock in Kühlungsborn, Ostseebad Kühlungsborn, Germany.

[2]Max-Planck-Institute for Solar System Research, Katlenburg-Lindau, Germany.


0148-0227/08/2007JD008875

[3] *Gadsden* [1985] was the first who found a 5-day periodicity in Noctilucent Clouds (NLCs) and suggested it might be related to 5-day waves, but he made no attempt to actually test his suggestion. Later on the impact of the 5-day wave on Polar Mesospheric Summer Echoes (PMSEs) and Noctilucent Clouds or Polar Mesospheric Clouds (PMCs) was investigated by *Kirkwood and Réchou* [1998], *Kirkwood et al.* [2002], *Merkel et al.* [2003], *von Savigny et al.* [2006], and *Riggin et al.* [2006]. In contrast to these authors, *Sugiyama et al.* [1996] proposed an internal quasi-limit cycle of 5-day duration assuming ice particles formation from proton-hydrates.

[4] A first attempt to model the 5-day wave was made by *Geisler and Dickinson* [1976] using mean zonal winds for the modeling. Later, *Salby* [1981] employed realistic winds. A numerical simulation of the 5- and 16-day waves was given by *Miyoshi* [1999]. The 5-day wave is a westward propagating Rossby wave with zonal wave number (1, 1). In the middle atmosphere the wave departs from its normal mode character in significant ways. It is marked by activity bursts and shows a pronounced phase tilt with altitude [*Riggin et al.*, 2006]. Such a strong outbreak of the 5-day wave activity was observed by Sounding of the Atmosphere using Broadband Emission Radiometer (SABER) in May 2003 [*Riggin et al.*, 2006].

[5] In this paper we calculate the dynamics and chemistry during the year 2003 on the basis of our new global 3D-model LIMA (Leibniz-Institute Middle Atmosphere model). The results are compared with water vapor measurements by means of the microwave technique carried out at ALOMAR observatory (69.29°N, 16.03°E), Norway. The goal of this paper is to investigate the influence of the 5-day wave particularly on the distribution of minor constituents within the mesosphere/mesopause region. In the second section we describe very briefly the ground-based radiometer used to measure the spectrum from the water vapor emission at 22.24 GHz, and the concept of our new model. The third section deals with the most important results for the high latitudes. The findings will be discussed in the fourth section, and in the final section we summarize the most important results.

## 2. Device and Brief Model Description

[6] The ground-based radiometer used for the water vapor measurements at 22.24 GHz as well as some results of the monitoring by the instrument system have been described by *Hartogh and Hartmann* [1990], *Hartogh et al.* [1991, 2004], *Hartogh and Jarchow* [1995], *Hartogh* [1997], and *Seele and Hartogh* [1999]. The microwave technique is an established tool to investigate the atmosphere with respect to certain measurable minor constituents such as water vapor or ozone. The vertical resolution of the water vapor retrievals depends on height and the signal-to-noise ratio of the measurements and ranges between about 5 and 10 km and the integration time is 1 day in the upper domain. The upper monitoring border is confined to 80 km. The uppermost panel is the most uncertain one and the inferred values could be somewhat underestimated. Water vapor has been measured at ALOMAR since 1995, with few interruptions. The year 2003 was selected because during the early summer season a strong outbreak of the quasi 5-day wave was observed [*Riggin et al.*, 2006].

[7] We use our new real-date GCM LIMA, a coupled model of the dynamics and chemistry, for the calculations. This model is briefly described by *Berger and Lübken* [2006], *Sonnemann et al.* [2006]. A more comprehensive description is under review. LIMA is a fully nonlinear global three-dimensional Eulerian grid point model extending from 0 to approximately 150 km with a vertical resolution of 1.1 km. The dynamic model has a completely new architecture, employing so-called simplex or three-angle coordinates (41804 horizontal grid points, a mesh size of approximately 110 km) advantageous for the gravity wave parameterization and the avoidance of the pole singularities. The main difference between the LIMA and its predecessor COMMA-IAP (Cologne Model of the Middle Atmosphere of the Institute of Atmospheric Physics, see also *Berger and von Zahn* [1999] or *Sonnemann and Grygalashvyly* [2005a], *Sonnemann et al.* [2006] and the quotations therein) is the fact that COMMA-IAP calculates climatological averages, whereas LIMA employs real tropospheric and lower stratospheric temperature and horizontal wind data up to 35 km altitude from the assimilation of ECMWF/ERA-40 (European Center for Medium Weather Forecast/Re-analysis Version 40) data. For the years before 2001 the model assimilates the ERA-40 data set [*Uppala et al.*, 2005], and since 2002 we use the operational data set of ECMWF. The atmospheric variability within the lower domain penetrates into the mesosphere/lower thermosphere (MLT-region) and results in a pronounced internal variability in the upper atmosphere. Additionally, for the calculations we apply real data of the Lyman-alpha flux according to *Woods et al.* [2000] (data available at: ftp://laspftp.colorado.edu/pub/SEE_Data/composite_lya/composite_lya.dat). That is the reasons to perform case studies by means of LIMA for a selected period and compare the model output with observed atmospheric parameters of the same period. In this way the model is able to calculate the propagation of planetary waves and can create sudden stratospheric warming events as shown by *Sonnemann et al.* [2006].

[8] The chemistry transport model (CTM) consists of three modules: chemistry, transport and the radiation module. It uses the dynamical fields of the temperature, the wind components and the pressure from the dynamical model. The CTM considers the advective transport and both the turbulent and molecular diffusion. We have adopted a time-independent eddy diffusion profile according to *Lübken* [1997]. This is certainly a restriction, but spatiotemporal eddy diffusion profiles are not yet available. We use a new a transport scheme according to [*Walcek*, 2000]. This scheme is marked by considerably reduced numerical diffusion. The chemical module is based on a family concept [*Shimazaki*, 1985] considering the odd hydrogen (H, OH, $HO_2$) and odd nitrogen (NO, $NO_2$, $N(^4S)$, $N(^2D)$) families. The odd oxygen constituents O and $O_3$ have been transported separately. This requires an integration time step not longer than 60 s.

## 3. Results

[9] Figure 1 shows the 7-day sliding average of the diurnal mean water vapor mixing ratio at ALOMAR

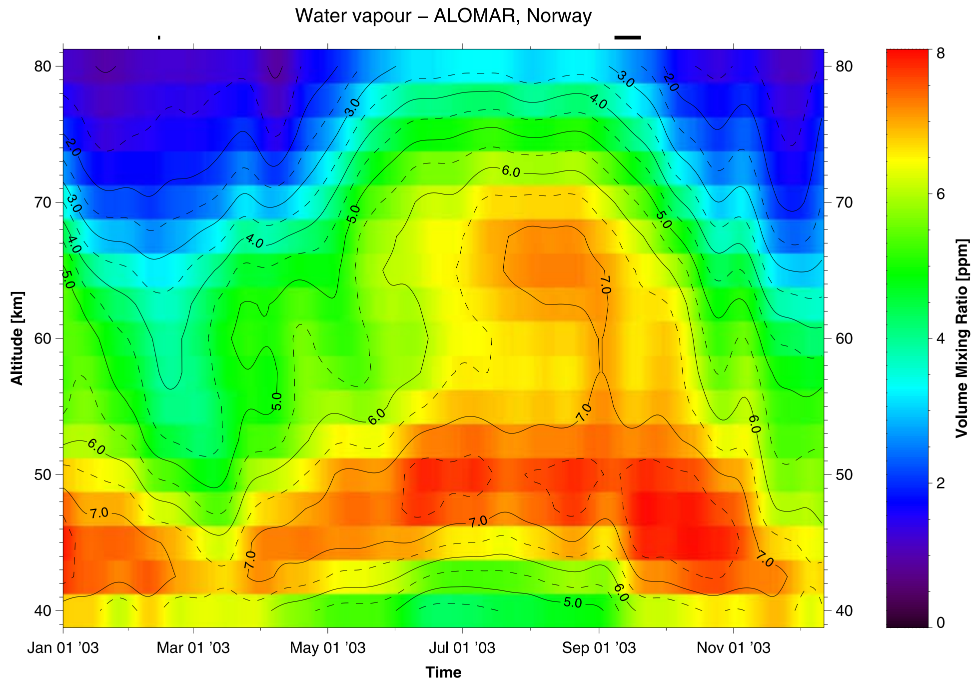


**Figure 1.** Seven-day sliding average of the diurnal mean water vapor mixing ratio at ALOMAR (69.29°N, 16.03°E), Norway between 40 and 80 km in 2003, measured by means of the microwave technique showing the annual variation marked by maximum values in late summer and minimum values in late winter/early spring.

between 40 and 80 km in 2003 measured by means of the microwave technique. The figure exhibits the well-known annual variation, with highest values in late summer and a strong increase from March to July. From the end of December 2002 through January and lasting until the end of February 2003, a strong water vapor enhancement occurred, resulting from a series of stratospheric warming events during the end of December 2002, the end of January 2003 and mid-February. These events were able to trigger the transport of water vapor. The annual minima of the water vapor mixing ratio occurred in early December and February/March. In summer a weak double maximum in altitude can be recognized, increasing toward late summer. The reason for this feature was discussed by *Sonnemann et al.* [2005]. It is a consequence of the auto-catalytic water vapor production connected with a meridional transport from the polar region. The averaging procedure smoothes out all oscillations with a period smaller than 7 days.

[10] Figure 2a displays the diurnally averaged water vapor mixing ratios for the period from May 1 to July 1, 2003 using a spline representation. A clear periodic variation of the water vapor mixing ratio can be recognized. In the middle to upper mesosphere, the absolute values strongly increase in the first half of May in accordance with the regular annual variation. The main maximum of the water vapor mixing ratio ranges close to the stratopause, with maximum values exceeding 7.5 ppmv. A second peak mostly occurs around 65 km. Between both maxima, a minimum establishes around 55 km. Although the mixing ratios decrease with increasing height the clearest quasi 5-day oscillation emerges at the upper monitored altitude at 80 km. Here the values vary between <2.5 and 4 ppmv whereas in the domain below, e.g., at a height of 70 km, the absolute variation only amounts to about 1 ppmv. The unsmoothed data for the diurnal mean water vapor mixing ratios during May 2003 are depicted in Figure 2b. The quasi 5-day oscillation is clearest above about 60 km.

[11] Figure 2c exhibits the variation of the water vapor mixing ratio after the summer solstice. The values are larger than in the period discussed previously and frequently exceed 8 ppmv around the stratopause. The periods of the variations are smaller than 5 days. At the secondary water vapor maximum, a quasi 2-day period is the most interesting feature in the second half of July. After that the period increases to 3–4 days in August.

[12] Figure 3 shows, according to Figure 1, a simulation by LIMA of the 7-day sliding mean of the diurnally averaged water vapor mixing ratio at 68.75°N, 16.875°E (close to the ALOMAR facility) in 2003 calculated by the real-date model LIMA. The model does a very good job of reproducing the annual variation, which includes special features like the stratospheric warming event, and the absolute values. However, the winter enhancement of the water vapor mixing ratio in the upper stratopause is smaller than the observations and the summer double peak is missing in 2003. Another deviation from the observations occurs in altitudes above 70 km, where the model values are higher than the measurements. We have already mentioned that possibly the mixing ratios of the observations are somewhat too small in the upper domain in summer, but we also cannot exclude that the upward transport of water vapor was somewhat too strong in the model in this year. Another cause of too large water vapor mixing ratio in the model output in the upper domain may be given by the fact that the model did not take into consideration a freeze drying in the area of PMSEs/NLCs.

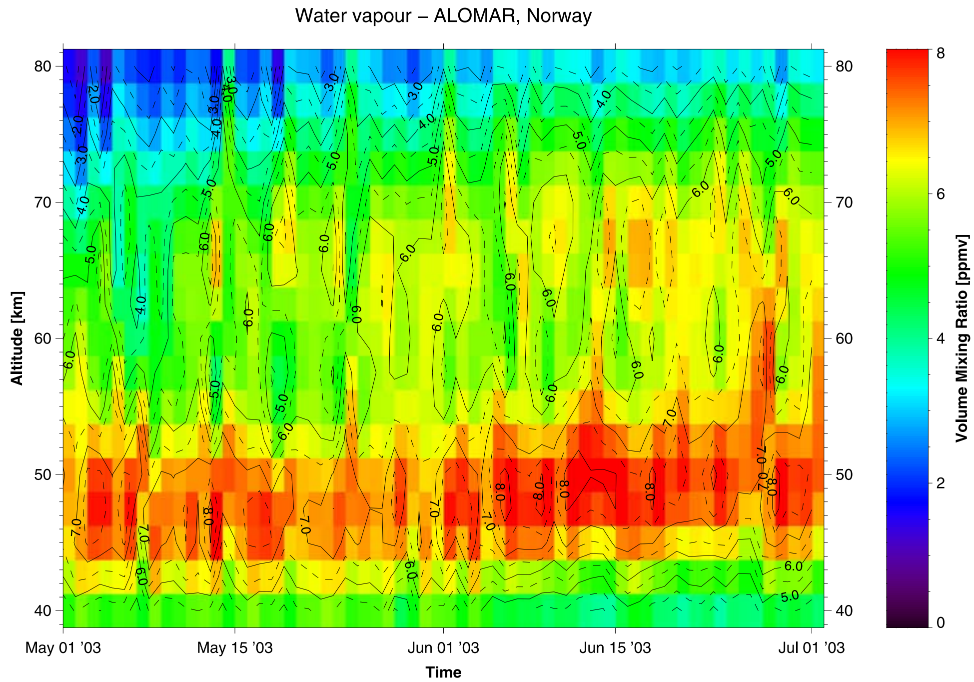


**Figure 2a.** The same state of affairs as shown in Figure 1 but for the time period May/June using a spline graphic representation.

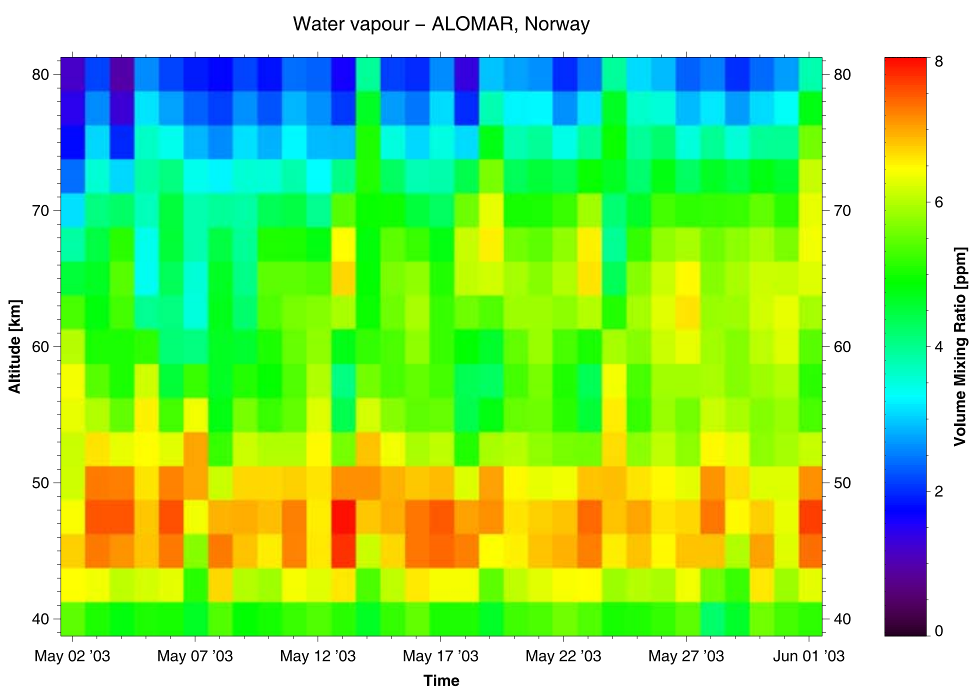


**Figure 2b.** The diurnal mean water vapor mixing ratios (unsmoothed) according to Figure 2a but only for May 2003, clearly displaying a quasi 5-day periodicity in the mesosphere.

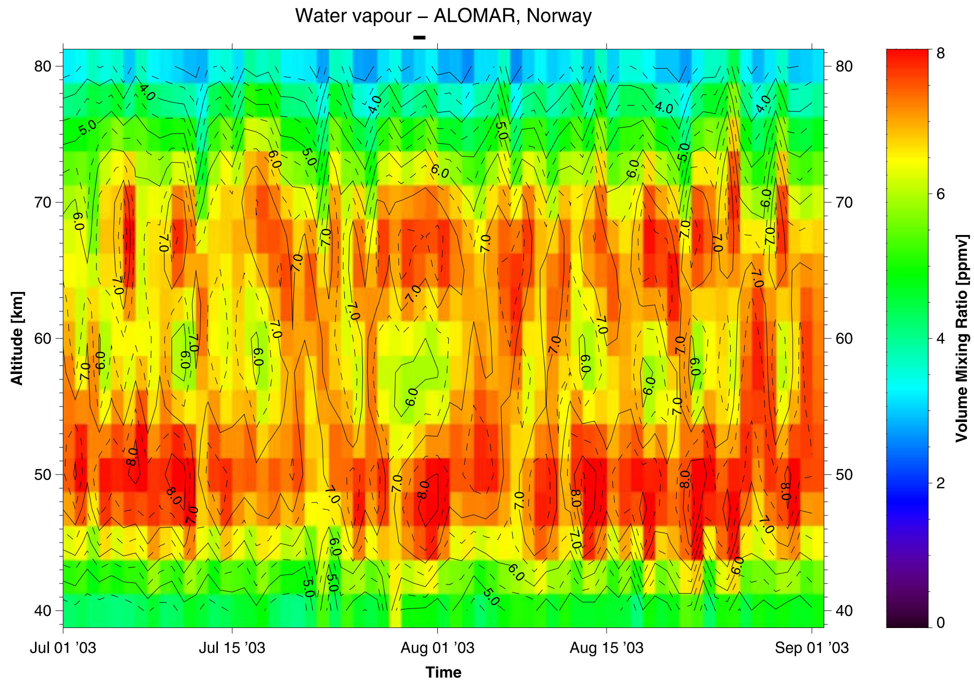


**Figure 2c.** The same state of affairs as shown in Figure 2b but for July/August. The black lines represent spline contours.

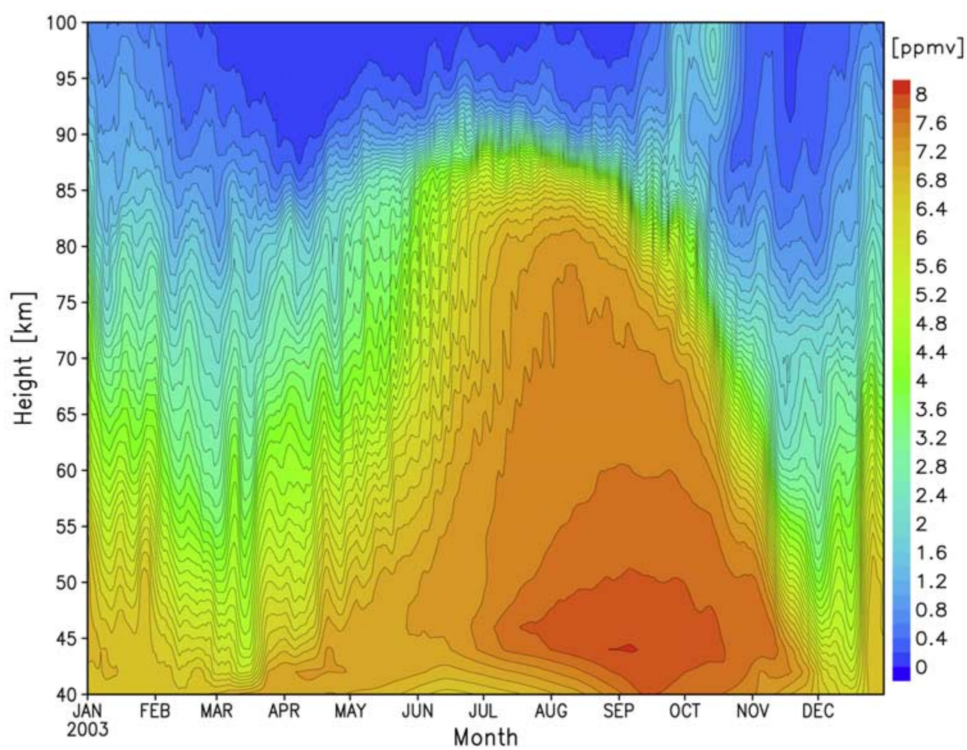


**Figure 3.** Seven-day sliding average of the diurnal mean water vapor mixing ratios at 68.75°N, 16.875°E (close to the ALOMAR facility) in 2003 calculated by LIMA.

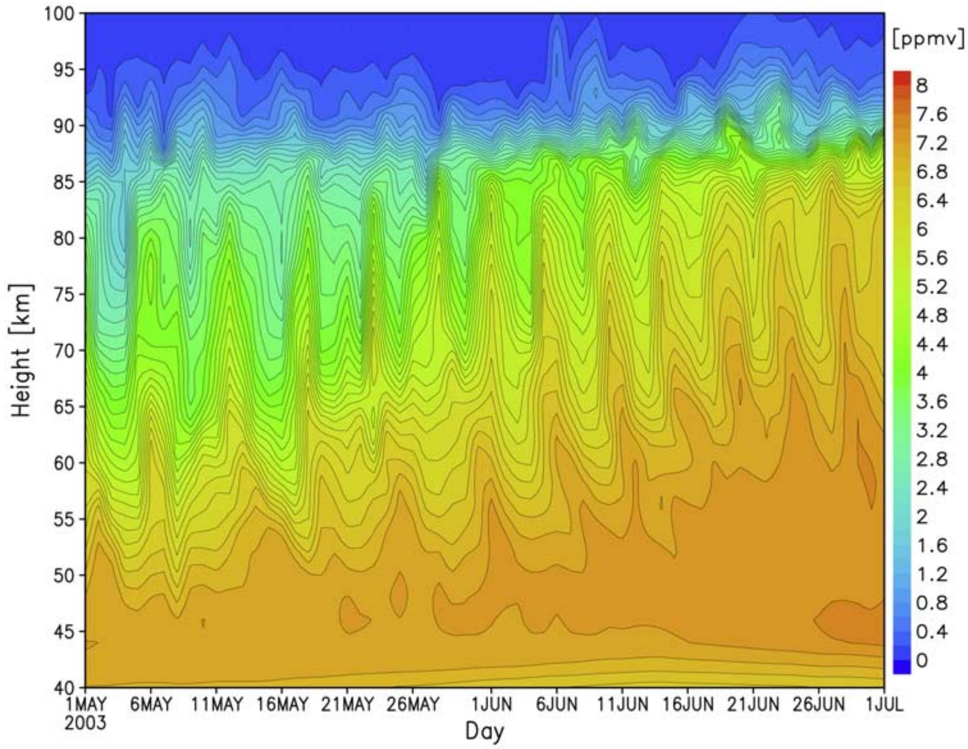


**Figure 4.** Diurnal mean water vapor mixing ratio at 68.75°N, 16.875°E for the same period as depicted in Figure 2a calculated by LIMA.

[13] Figure 4 displays the same state of affairs as shown in Figure 3 but for the period May/June 2003. Apart from the general increase of the water vapor mixing ratio due to the regular annual enhancement toward the summer solstice, the model output shows a rather clear quasi 5-day oscillation in the upper domain over the whole period. In the domain below about 70 km a 7-day period frequently occurs interrupted by 5-day oscillations, so that an average period of about 6 days results. In July and August a 5-day variation is still recognizable in the NLC region (not shown) but with a considerably reduced amplitude. In contrast to Figure 2c, a clear indication for a quasi 2-day wave was not found in the model data. Perhaps this wave could be triggered by a 2-day oscillation of the chemical heating rate between 80 and 90 km, as found and discussed by *Sonnemann and Grygalashvyly* [2005b], which was not taken into calculation by LIMA. Figure 5 compares the water vapor mixing ratios measured at ALOMAR (black line) and calculated by LIMA (red line) at an altitude of 70 km for the period between April 15 and June 15. 70 km is the height of reliable measurements. Both curves reflect the seasonal increase of the water vapor mixing ratio. The dates of maxima agree in general within a 1 day uncertainty. Note that both the observations and calculations represent diurnal averages.

[14] Figure 6 displays the deviation of the diurnal mean of the water vapor mixing ratio from an average taken from 21 March to 16 May showing the start of the quasi 5-day wave at the beginning of May. A first oscillation already occurs approximately ten days before the onset of the 5-day wave during the end of April/beginning of May. Figure 7a exhibits a latitudinal section of the diurnal mean water vapor mixing ratio at an altitude 74 km for the period from 1 May to 1 July 2003. The figure demonstrates that the effect is confined to summer high (with exclusion of the polar area) and middle latitudes. The wave is most pronounced around 60°N at this height. In the southern

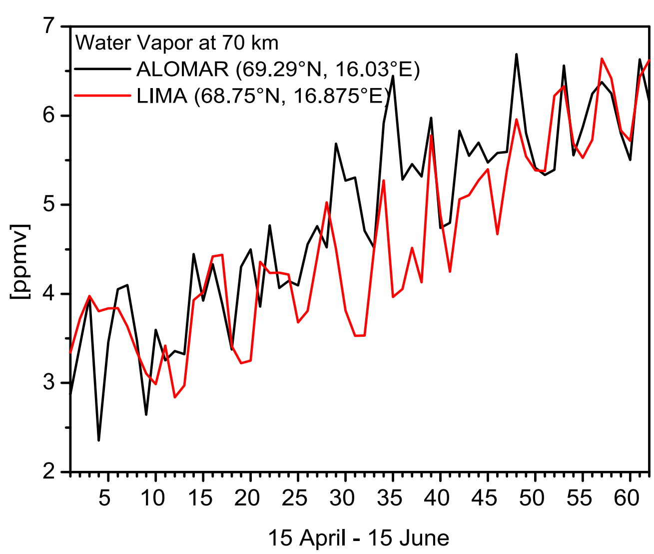


**Figure 5.** Comparison between the water vapor observations in ALOMAR (black line) and the calculations by LIMA (red line) at 70 km for the period 15 April to 15 June 2003. Both the absolute values and the variations agree quite well.

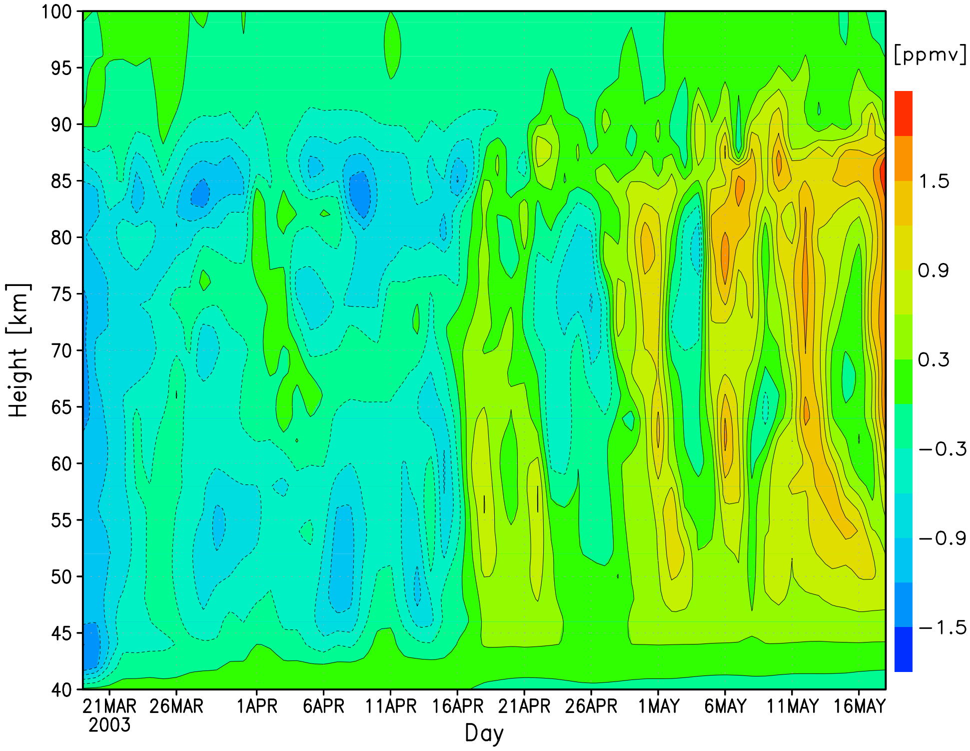


**Figure 6.** Deviation of the diurnal mean water vapor mixing ratio from an average in the considered period 21 March to 16 May 2003 showing the start of the quasi 5-day wave at the beginning of May. A first oscillation already occurs approximately ten days before the onset of the 5-day wave.

hemisphere a similar variation occurred half a year later, but the effect is not as pronounced at this height, at least in 2003, as Figure 7b makes clear. Generally, in the upper mesosphere, the water vapor mixing ratios are larger in the southern hemisphere during the summer season than that ones in the northern hemisphere for the corresponding season. We found the same asymmetry in calculations based on our climatological mean model COMMA-IAP. Also, the HALOE water vapor measurements (http://haloedata.larc.nasa.gov/home/index.php) revealed an asymmetry of approximately 10 % between southern summer and northern summer above 65 km. The reason of this asymmetry is not completely clear thus far and may be connected with the fact that the Earth's orbit is closer to the Sun during the southern summer than during the northern summer. However, the strongest influence on the water vapor distribution should have the asymmetric circulation on both hemispheres [*Lübken et al.*, 2004]. Test runs by means of COMMA-IAP using symmetric wind fields in the CTM result in almost no differences between both hemispheres during the same season.

[15] The whole year shows wavelike features in the water vapor mixing ratio reflecting different dynamical processes in the atmosphere. Figure 8 displays the deviation of the water vapor mixing ratio from a 14-day sliding mean measured at ALOMAR for all available data in 2003 in a height-season section. Bold black bars at the top indicate observation gaps. The data within the gaps have been linearly interpolated. Although the absolute water vapor concentrations are essentially smaller during the winter season, the absolute deviations are in the same order as in the summer season. Also, the model output shows pronounced oscillations in winter, particularly in connection with sudden stratospheric warming as discussed by *Sonnemann et al.* [2006] on the basis of LIMA calculations. However, the types of waves are different between summer and winter. During winter the wave activity in the MLT region is determined by penetration of planetary waves with zonal wave numbers 1 to 3 propagating from the troposphere through the winter tropopause under the condition of a not too large westerly wind [*Charney and Drazin*, 1961; *Dickinson*, 1968]. During summer, waves coming from the troposphere are trapped in regions where the zonal wind is easterly [*Charney and Drazin*, 1961; *Dickinson*, 1968]. In this case the waves in the MLT region are internal waves which most probably originate due to baroclinic or barotropic instabilities or they are a mixture of both [*Meyer and Forbes*, 1997].

## 4. Discussion

[16] As stated by *Riggin et al.* [2006], the year 2003 was marked by a strong appearance of the quasi 5-day wave in the northern hemisphere, particularly in May. This statement has been confirmed by our results. We have considered further available years (not shown here) and found generally a similar behavior of wave activity. The inspection of the variation by eyes revealed differently long periods. In order to analyze the observation as well as the model output with respect to the wave periods, we used the fast Fourier transform (FFT) method [*Julian*, 1971]. Figure 9a shows an example for the ALOMAR water vapor data at different

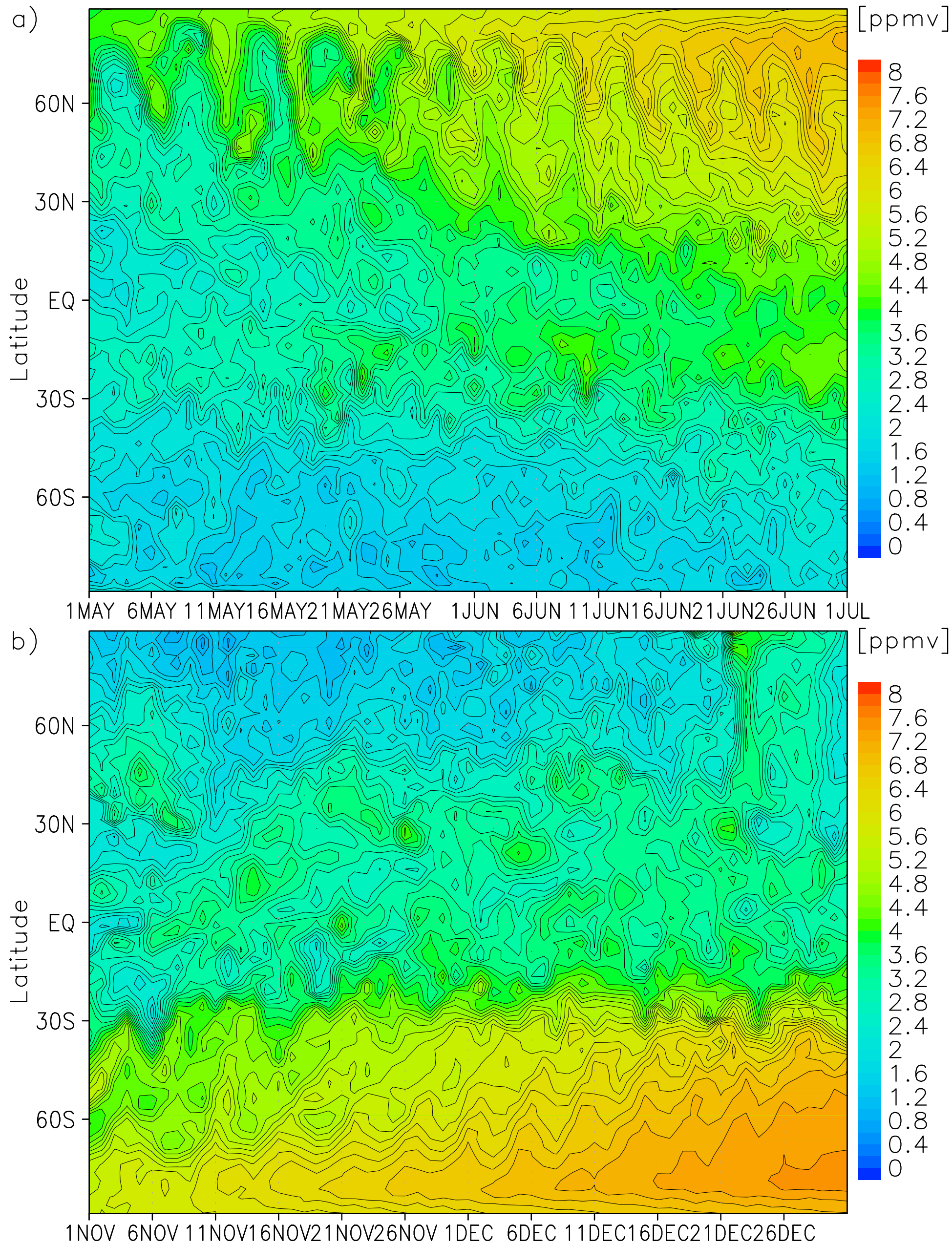


**Figure 7.** (a) Latitudinal section of the diurnal mean water vapor mixing ratio at 74 km altitude for the period May/June, 2003. The figure demonstrates that the effect is confined to high (with exclusion of the polar area) and middle latitudes. (b) According to Figure 7a the same section, but shown a half year later. The effect is not as pronounced at this height as in the northern hemisphere a half year before.

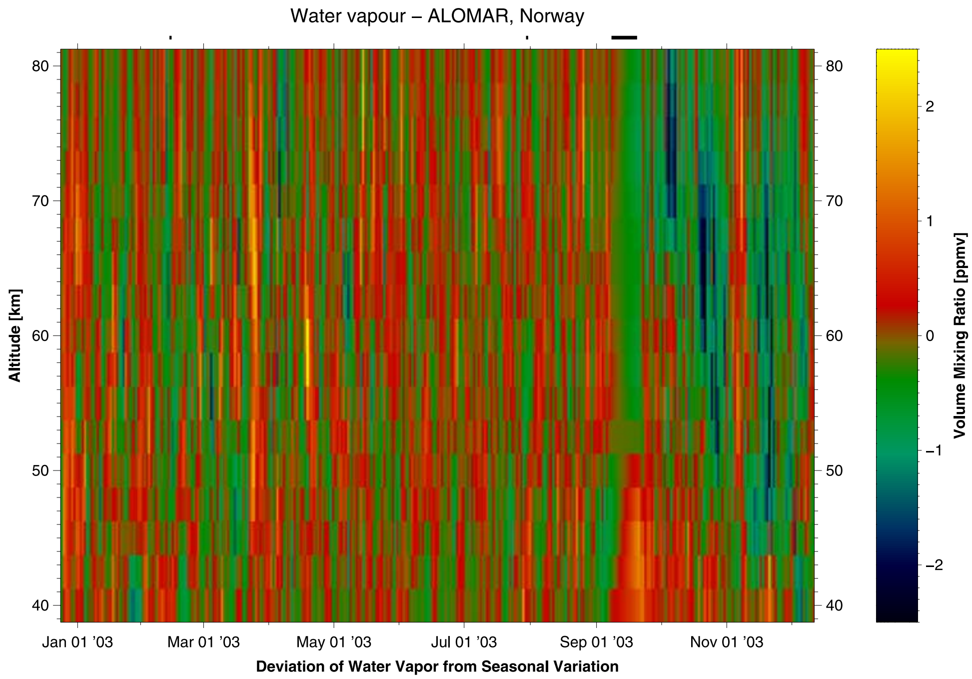


**Figure 8.** Deviation of the diurnal mean water vapor mixing ratio from the 14-day sliding average at ALOMAR for all available observations in 2003 showing pronounced wavelike features over the whole year. The bold black bars at the top indicate gaps of observations. The data within the gaps have been linearly interpolated.

height levels between 15 April and 15 June 15. A peak occurs for all heights at about 4.6 days; another peak occurs at about 5.3 days. A third maximum occurs (at least for the 60 and 70 km levels) at about 7 days. The same analysis performed for the LIMA data revealed a somewhat different picture, as shown in Figure 9b. This figure (as well as Figure 9a) displays two most pronounced maxima with periods near 5 days. The first maximum has a period of 4.6 days (as well as the result of measurements) at 50 and 60 km. It shifts with increasing altitude to 4.9 days at 70 and 80 km. The second maximum inferred from the calculations and likewise derived from the measurements has a period longer than 5 days and ranges at 5.8 days at 70 and 80 km. The period is shifted to 6.4 days at 60 and 50 km.

[17] The effective lifetime of water vapor below 80 km is extremely long and is essentially longer than 5 days [*Körner and Sonnemann*, 2001; *Sonnemann et al.*, 2005]. Consequently, the variation of the water vapor concentration is determined by transports. A vertical transport triggered by the quasi 5-day wave can convey dry air from above or wet air from below. This seems to be the dominant process in the upper domain. However, the secondary maximum at the height of 65 km cannot be interpreted in terms of vertical transport only, but it can also have been triggered by a meridional transport along the meridional water vapor gradient with increasing mixing ratios toward the pole. The observations display this double maximum structure more clearly than the calculations. For the latter, such a feature occurs only during the positive phase of the quasi 5-day wave. The averaging procedure, as used for Figure 3, smoothes out these features only in 2003, whereas the feature occurs in higher latitudes and in other years in late summer [*Sonnemann et al.*, 2005]. A meridional wind blowing from the pole (negative values) transports more humid air toward the south. As higher water vapor values at the secondary maximum are connected with lower values 10 km below, the meridional wind should at least change its magnitude.

[18] Figure 10a exhibits the diurnal mean meridional wind during May 2003. The quasi 5-day wave can be clearly recognized. A strong event of positive meridional winds occurs for instance between 9 May and 11 May. A tilt of the phase of approximately two days can be noticed between heights of 80 and 40 km. Such a downward phase progression was also found by *Wu et al.* [1994] and by *Riggin et al.* [2006], the latter using SABER temperature data. The secondary maxima of water vapor are more or less connected with negative meridional wind; however, the picture is more complicated, as the trajectory of a moving air parcel also influenced by the zonal wind must be considered. The pronounced oscillation of the meridional wind in the model may also prevent the formation of the secondary water vapor maximum in the summer season. Figures 10b and 10c display the corresponding diurnal mean zonal and diurnal mean vertical wind components. All wind components are marked by a quasi 5-day oscillation, but less clearly for the vertical wind component. The zonal wind is generally negative below 85 km and ranges in the order of some 10 m $s^{-1}$ depending on height. It belongs to the summer easterly wind regime not yet fully established during the period considered. The periods of strongest zonal wind are connected with negative meridional wind. The amplitude of the 5-day oscillation amounts to some m $s^{-1}$. The vertical wind also changes its sign. In the upper mesosphere the water vapor mixing ratio possesses a strong vertical gradient. The vertical wind modulates the water

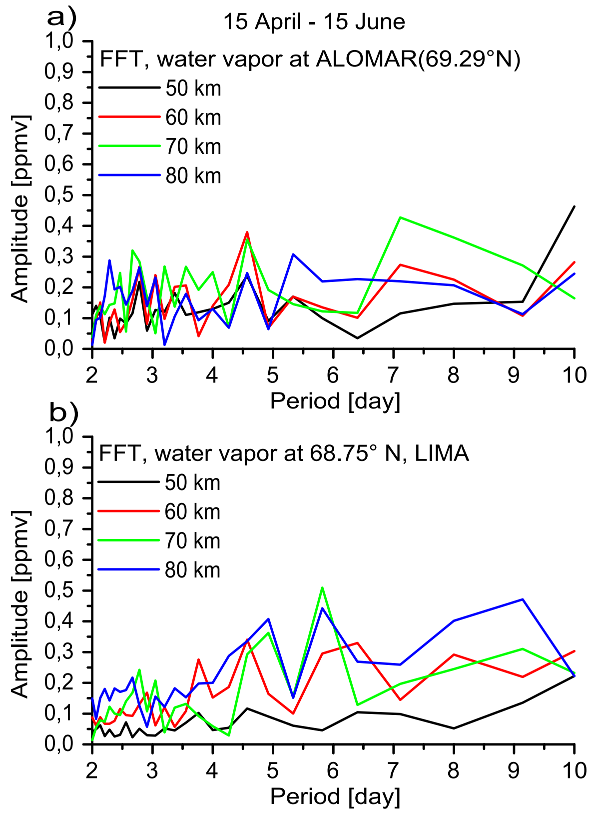


**Figure 9.** (a and b) Fast Fourier transform analysis of the water vapor mixing ratio in different heights for the period 15 April to 15 June 2003. Figure 9a displays the analysis of the ALOMAR observations and Figure 9b the corresponding LIMA data. Around a period of 5 days the amplitudes possess a split peak.

vapor mixing ratio accordingly, as can be clearly recognized in the upper domain (see Figures 2a to 2c) of the ALOMAR measurements.

[19] The most important parameter for the formation of PMSEs and NLCs is the temperature, but it also influences the ozone formation. The temperature shows the same periodicity as the wind and water vapor data. Figure 11a displays midnight values of the temperature (bold curve) and the water vapor mixing ratio (thin curve) at the same latitude and longitude as considered before at 86 km (close to the mesopause height) from 1 May to 1 August 2003. The figure exhibits the seasonal variation, with coldest temperatures and highest water vapor mixing ratios after solstice. The quasi 5-day variations are not as clear compared with the region below. A tendency of anti-correlation can be found at this latitude, meaning that the variation of water vapor supports the variation of the formation of NLCs triggered by the temperature. The influences of planetary waves and especially of the temperature on the occurrence rate of NLCs were investigated by *Kirkwood and Réchou* [1998], *Kirkwood et al.* [2002], *Merkel et al.* [2003], *von Savigny et al.* [2006], and *Riggin et al.* [2006], whereas *Sugiyama et al.* [1996] proposed an internal quasi limit cycle of 5-day duration including ice particles formation on proton-hydrates, their sedimentation and then evaporation at the lower border of NLCs.

[20] Figure 11b shows the same state of affairs as in Figure 11a, but at 76.25°N. Now the variation is not so clear and sometimes both parameters vary in phase, meaning that water vapor damps in this case the influence of the varying temperature in limited borders. The difference between maximum and minimum values of the temperature ranges in the order of two to four degrees and that of the water vapor mixing ratio of about one ppmv. The figures make clear that the variation of the temperature is absolutely able [*Kirkwood and Réchou*, 1998] to modulate the occurrence rates of NLCs (PMCs) and PMSEs.

[21] The variation of ozone is less clear. Generally, decreasing temperatures and water vapor concentrations increase the ozone concentration. The reason is well-known and consists in the fact that water vapor is the source of hydrogen radicals which destroy ozone. The chemical reaction rates for decreasing temperature act in the direction of ozone enhancement and the ozone loss takes place by reactions with hydrogen radicals resulting from the photolysis of water vapor. The characteristic time of the odd oxygen system increases with height so that, particularly in the mesopause region and above, ozone will be strongly influenced especially by vertical transport. In case where water vapor and the temperature vary opposite, the influences partly compensate one another. As introduced by *Sonnemann* [2001] and discussed for a realistic model by *Sonnemann and Grygalashvyly* [2003], the zonal wind has a considerable influence on the diurnal variation of ozone. The investigation of this so-called photochemical Doppler-Sonnemann effect was extended, and particularly the anomaly of the night-to-day ratio (NDR) of ozone in winter was interpreted in terms of this effect [*Sonnemann et al.*, 2007]. It was found that the zonal wind strongly influences the nighttime ozone level during the sunset period. The reason is that the winter zonal wind blowing in the direction of the Earth's rotation shortens the time of sunset. During this time the largest odd oxygen loss takes place when atomic oxygen is transformed into ozone. The net odd oxygen production from the dissociation of molecular oxygen is stopped under the condition of large solar zenith angels, but the photolysis of ozone continues further. On the one hand, $O(^1D)$ resulting from ozone dissociation can oxidize water vapor, thereby forming hydrogen radicals. On the other hand, atomic oxygen formed by the quenching of $O(^1D)$ can directly react with ozone. Thus a shortening of the time of sunset relatively enhances the nighttime ozone level. A summer easterly wind prolongs the time of sunset for a moving air parcel compared with one under zero wind conditions. Thus a reduced zonal wind velocity increases ozone relatively to normal wind conditions. During the daytime, an easterly wind system also prolongs the time of ozone formation, resulting in an altered diurnal variation.

[22] *Rosenlof and Thomas* [1990] found a 5-day wave in mesospheric daytime ozone data measured by the Solar Mesosphere Explorer (SME) satellite in high southern summer (December) latitudes. The amplitude, however, was relatively small and amounted to only a few percent. Figure 12 shows the nighttime average of the ozone mixing ratio at a height of 76 km in high southern latitudes around solstice for the south summer 2002/03. One can see a quasi

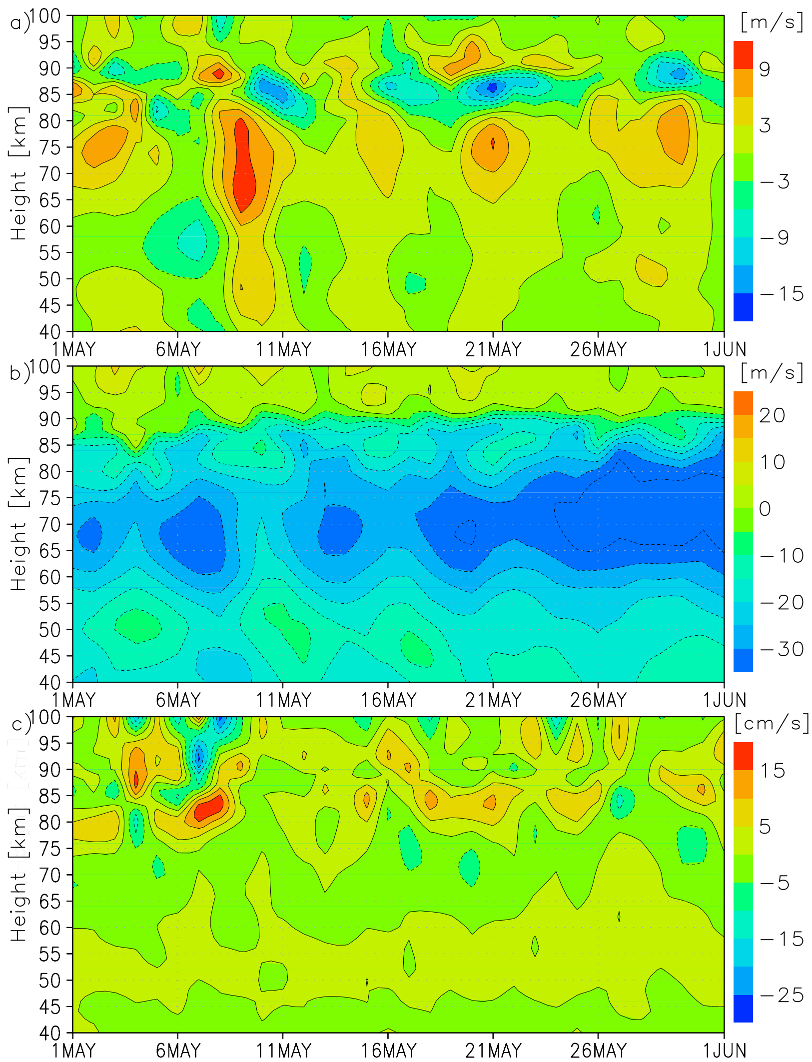


**Figure 10.** The diurnally averaged meridional (a), zonal (b) and vertical wind component (c) at 68.75°N during 1 May to 1 June 2003 calculated by LIMA. The zonal and meridional winds show the clearest wavelike features.

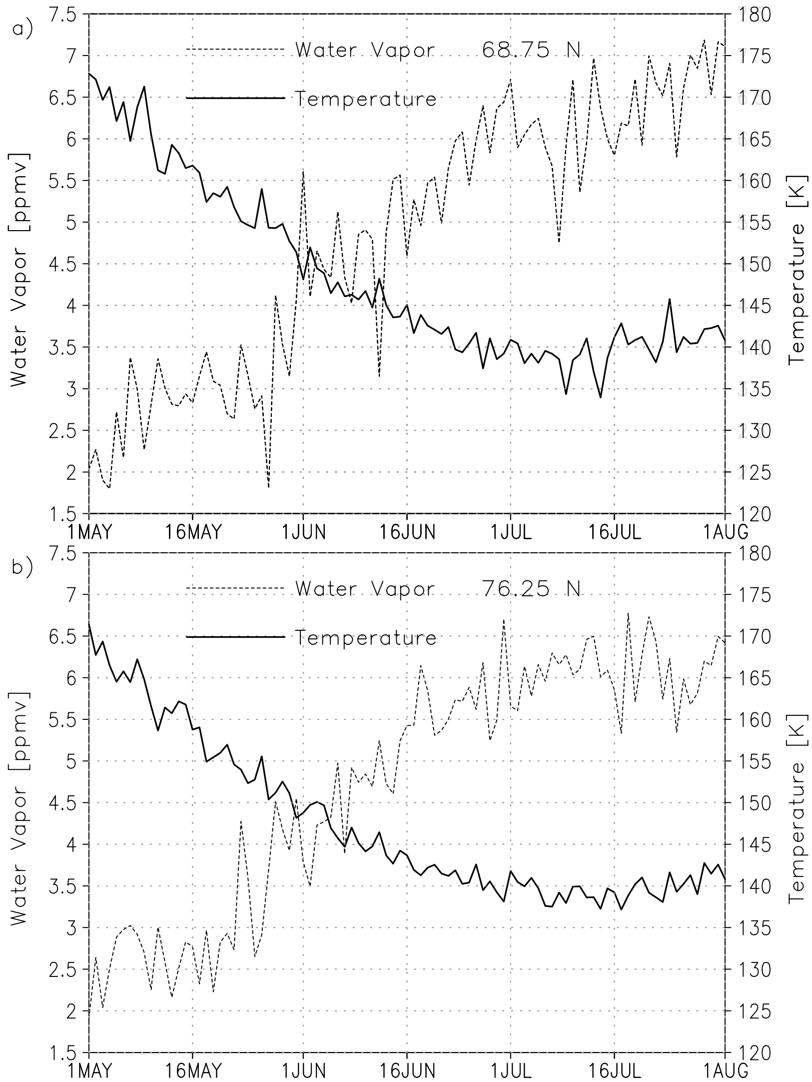


**Figure 11.** Midnight values of the water vapor mixing ratio (thin) and temperature (bold) at 68.75°N (a) and at 76.25°N (b) at 86 km altitude from 1 May to 1 August 2003. The seasonal variation is just opposite. Decreasing temperatures are linked up with increasing water vapor mixing ratios.

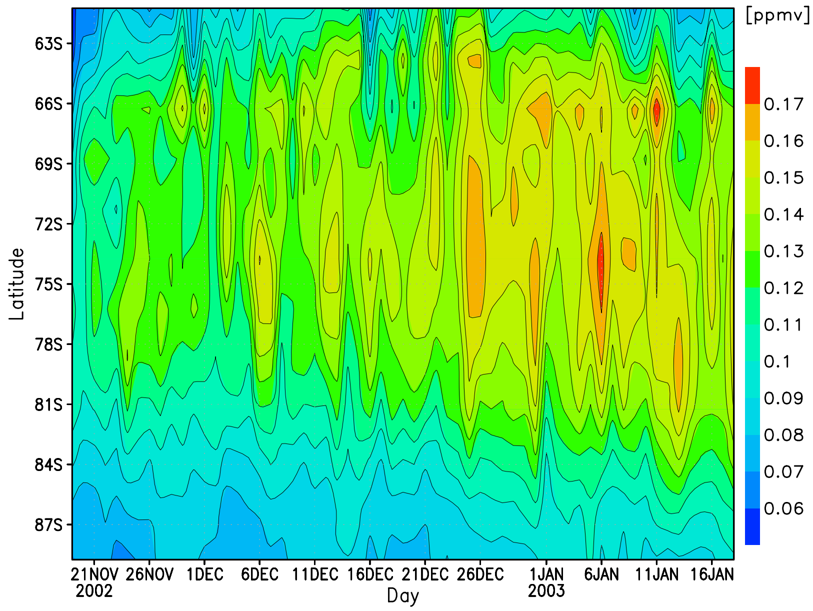


**Figure 12.** Midnight values of the ozone mixing ratio at 76 km displayed in a latitude-time section around southern summer solstice in 2002/3 calculated by LIMA. The figure shows a quasi 5-day period. The amplitude ranges in the order of 10 %.

5-day oscillation with an onset at the beginning of December. The amplitude does not exceed 10 %, as also found by *Rosenlof and Thomas* [1990]. In latitudinal region beyond about 80°S, ozone varies more irregularly. Figure 13a displays an example for a quasi 5-day oscillation in the northern hemisphere. The figure compares the temperature, water vapor mixing ratio and ozone concentration and the zonal wind at 64 km and at 68.75°N at midnight during May 2003. Surprisingly, ozone and water vapor are positively correlated. The temperature is also weakly positively correlated with the first quantities, but the variation is too small to entail a marked ozone variation. This finding means that the variation of both species can only be triggered by the winds. Figure 13b depicts the same state of affairs but at 74 km. The variations seems to indicate an anti-correlation between ozone and the temperature, however, the variations of all depicted parameters are not very clear. We have to keep in mind that ozone values at a fixed local time are unable to characterize the general behavior of ozone because ozone is marked by a distinct diurnal variation. The diurnal variation becomes more pronounced with increasing height and has, in contrast to that at 64 km, a noticeable amplitude at 74 km.

[23] The latitude of 68.75° is already beyond the polar day terminator during summer solstice. Considering a latitude beyond the polar day area and averaging the ozone values over the day, the ozone variations become small in the mesosphere. Figure 14a displays the results at 61.25° for 9 June to 27 June 2003. The variations are very small and in the order of magnitude shown in the paper of *Rosenlof and Thomas* [1990] but they are not negligible in the upper domain. An amplitude increasing with height also agrees with the findings of *Rosenlof and Thomas* [1990]. The result is more interesting when we consider the night-to-day ratio of ozone (Figure 14b). We define as the nighttime value the average between sunset and sunrise, and as the daytime value the mean between sunrise and sunset of the following day. The structure of the quasi 5-day oscillation is best visible around 73 km, although the amplitude is relatively small. Thus in spite of small variations in the absolute values of ozone, the NDR can serve as an indicator of wave activity. The water vapor distribution for this case is shown in Figure 14c. The figure displays the same periodicity and the downward progression of the phase. Larger values of the NDR are more or less coupled with daytime ozone minima but the connection to the water vapor mixing ratio is not so clear. For the first two periods, high NDR are connected with large water vapor mixing ratios, but the situation is opposite for the following two periods. This indicates that further influences, such as the temperature, have a say in the matter.

[24] In the height of the secondary ozone maximum at 85 to 90 km, the variations of the NDR are rather strong as Figure 15a makes clear for the period from 27 June to 9 July 2003. In this domain the variation essentially depends on the downward transport of atomic oxygen and atomic hydrogen. Figure 15b shows the atomic oxygen concentration at midnight and Figure 15c displays the ozone concentration averaged over the night. A large downward transport of atomic oxygen entails both large daytime and nighttime ozone values so that the NDR is not so strongly influenced by this transport. In contrast to this, the reaction with atomic hydrogen is the dominant loss for ozone during the night when the photolysis is zero, whereas during the daytime photodissociation is the main sink for ozone. The photodissociation is almost constant in this domain during the daytime. Figure 15d depicts the atomic hydrogen concentration. High values of the NDR are connected with large nighttime ozone concentrations and with small atomic hydrogen concentrations triggered by vertical transport.

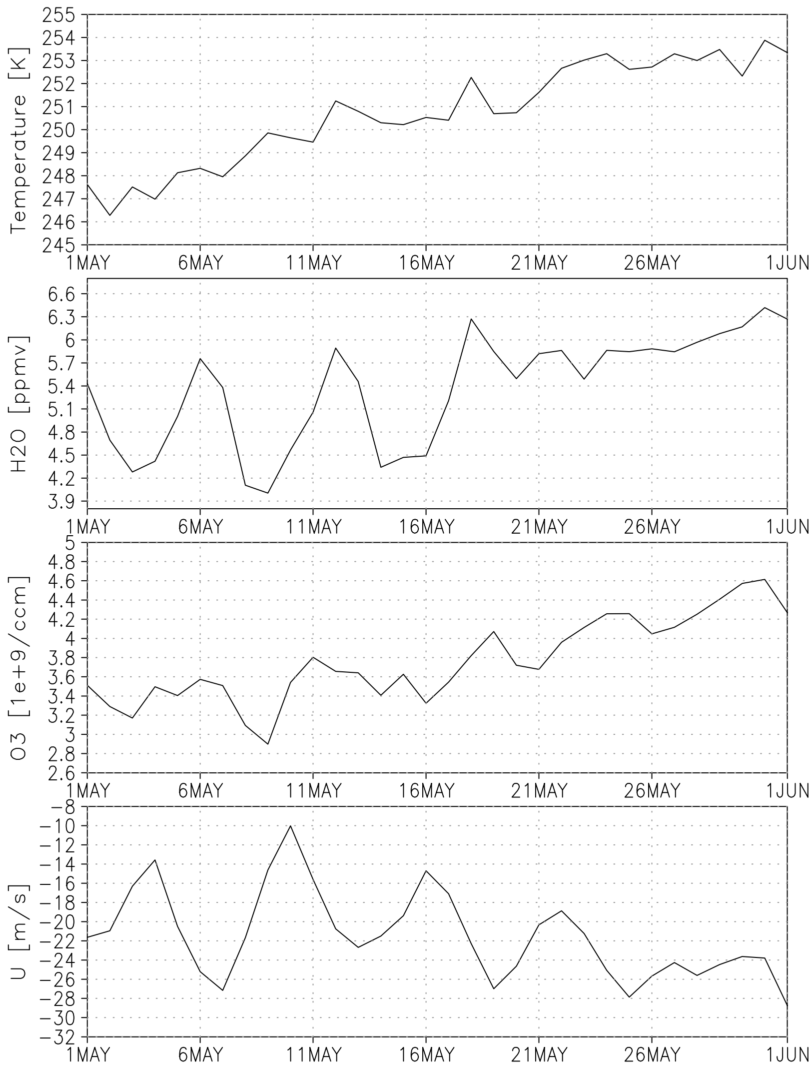


**Figure 13.** Comparison of midnight values of the temperature, water vapor mixing ratio, ozone concentration, and the zonal wind at 64 km (a) and 74 km (b) at 68.75°N during May 2003 calculated by LIMA. The clearest oscillations show the water vapor mixing ratio and the zonal wind.

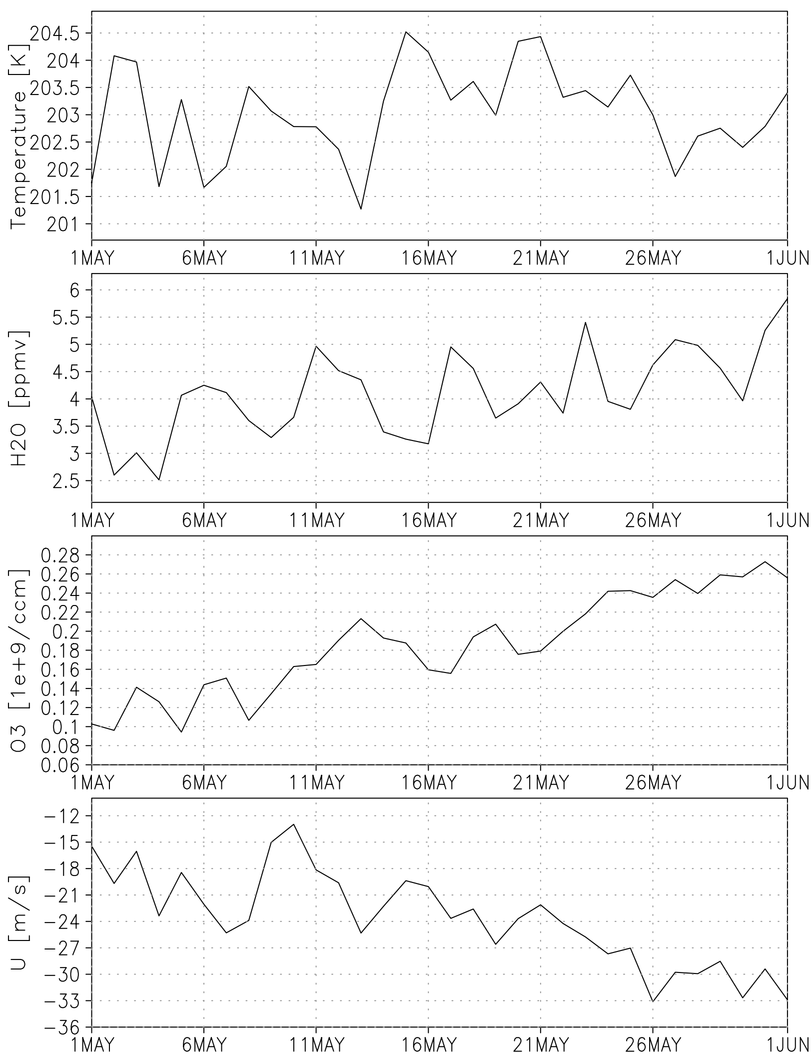


**Figure 13.** (continued)

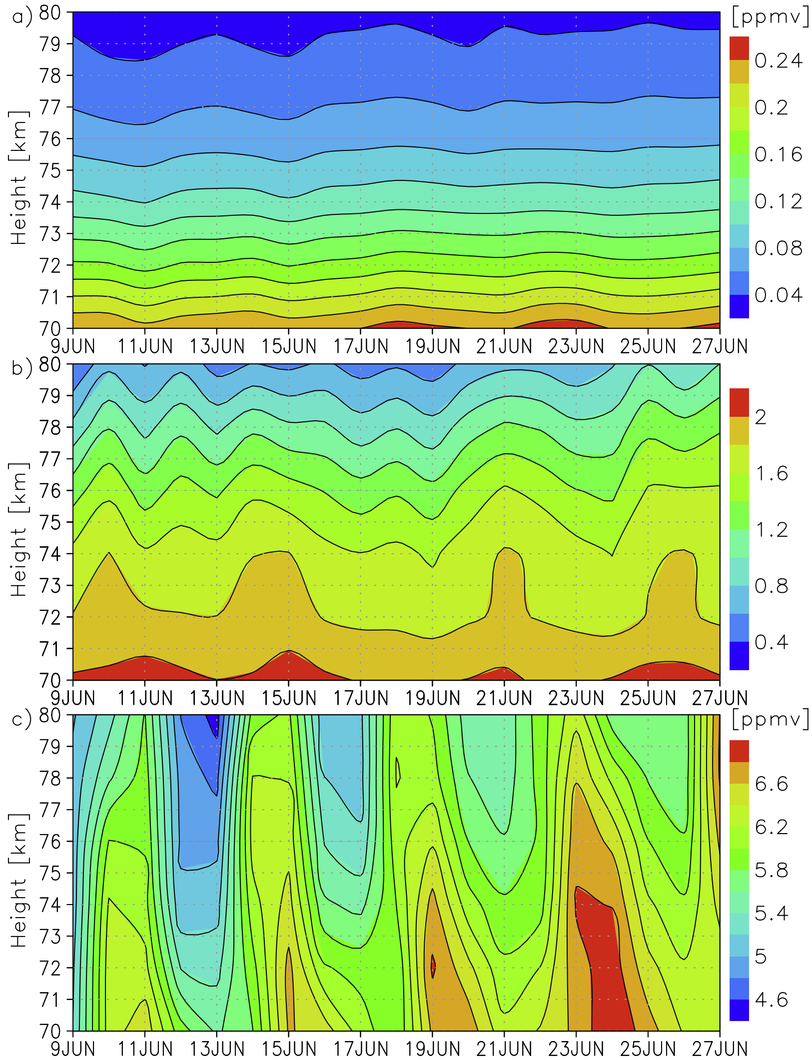


**Figure 14.** (a to c) Variation of the mean daytime ozone mixing ratio, the night-to-day ratio of ozone, and the water vapor mixing ratio in a height-time section at 61.25° from June to July 2003 calculated by LIMA. The variation of ozone is relatively small whereas its night-to-day ratio and the water vapor mixing ratio show clear quasi 5-day oscillations.

Ozone rises after the increase of atomic oxygen but the peak concentration also depends on the loss by reaction with atomic hydrogen ($[O_3] \sim [O]/[H]$). The ozone peaks are located below the atomic oxygen peaks due to the fact that the ozone formation depends quadratically on the air density increasing exponentially with decreasing height. In the domain of the secondary ozone maximum the variation of the atomic hydrogen concentration is mainly determined by transport and not by the photolysis of water vapor. This statement is verified by the fact that phases of large atomic hydrogen concentrations are correlated with minimum water vapor mixing ratios, indicating a downward transport of atomic hydrogen, but it is connected with a transport of dry air.

## 5. Summary and Conclusions

[25] The analysis of the water vapor measurements in 2003 by means of the microwave technique in high latitudes at ALOMAR, Norway, revealed the signature of a quasi 5-day wave in the mesosphere beginning in May and lasting with decreasing amplitude until mid-July. Afterward until the end of August smaller periods dominated. The period really varies between about 5 and 7 days but it decreases to 2 to 4 days after mid-July. Real-date calculations on the basis of the GCM LIMA brought evidence that the 5-day wave is a phenomenon occurring particularly in high and middle latitudes during the summer season. The agreement of the calculations with the observations is relatively good, although some differences also occur. These waves were theoretically predicted by *Geisler and Dickinson* [1976] and *Salby* [1981, 1984] and identified as a normal (1, 1) mode Rossby wave. The dynamical parameters (wind components and temperature) are able to modulate the transport of relatively inert minor constituents such as water vapor in the whole middle atmosphere, and atomic hydrogen and atomic oxygen in the lower thermosphere. They also impact

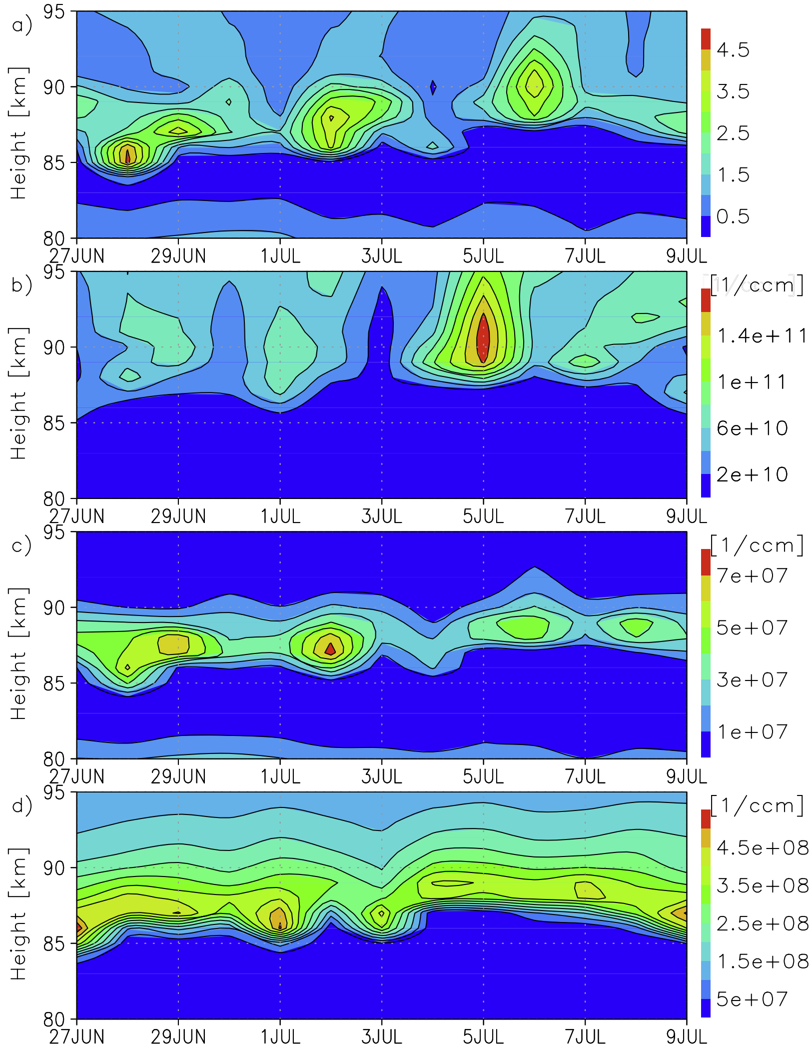


**Figure 15.** (a to d) Night-to-day ratio (NDR) of ozone, the atomic oxygen, the ozone, and the atomic hydrogen concentrations, within the mesopause region at 61.25°N for a period in June/July 2003 calculated by LIMA exhibiting a pronounced quasi 5-day oscillation at 85–90 km altitude. Large values of the NDR are connected with small atomic hydrogen concentrations.

the chemistry of constituents marked by characteristic times noticeably smaller than 5 days. The variation of both the temperature and the water vapor mixing ratio influences the occurrence rates of NLCs and PMSEs. The calculations show a strong influence of the NDR of ozone in the height of the secondary ozone maximum, whereas the impact on the mesospheric ozone is relatively small. The year 2003 was marked by a strong outbreak of the quasi 5-day wave. The analysis of further years of water vapor measurements at ALOMAR has yet to be done.

[26] **Acknowledgments.** The work was supported by Deutsche Forschungsgemeinschaft, project HA 3261/1-2 and So 263/4-1.

## References


Berger, U., and F.-J. Lübken (2006), Weather in mesospheric ice layers, *Geophys. Res. Lett.*, *33*, L04806, doi:10.1029/2005GL024841.

Berger, U., and U. von Zahn (1999), Two level structure of the mesopause: A model study, *J. Geophys. Res.*, *104*, 22,083–22,093.

Charney, J. G., and P. G. Drazin (1961), Propagation of planetary scale disturbances from the lower into the upper atmosphere, *J. Geophys. Res.*, *66*, 83–109.

Dickinson, R. E. (1968), On the exact and approximate linear theory of vertically propagating planetary Rossby waves forced at a spherical lower boundary, *Mon. Weather Rev.*, *96*, 405–415.

Fraser, G. J. (1977), The 5-day wave and ionospheric absorption, *J. Atmos. Terr. Phys.*, *39*, 121–124.

Fraser, G. J., and M. R. Thorpe (1976), Experimental investigations of ionospheric/stratospheric coupling in southern mid latitudes-1. Spectra and cross-spectra of stratospheric temperatures and the ionospheric f-min parameter, *J. Atmos. Terr. Phys.*, *38*, 1003–1011.

Gadsden, M. (1985), Observations of noctilucent clouds from North-West Europe, *Ann. Geophys.*, *3*, 119–126.

Geisler, J. E., and R. E. Dickinson (1976), The five-day wave on a sphere with realistic zonal winds, *J. Atmos. Sci.*, *33*, 632–641.

Hartogh, P. (1997), High resolution chirp transform spectrometer for middle atmospheric microwave sounding, In J.D. Haigh, editor, Satellite Remote Sensing of Clouds and the Atmosphere II, *Proc. SPIE*, vol. 3220, 115–124.

Hartogh, P., and G. K. Hartmann (1990), A high resolution chirp transform spectrometer for microwave measurements, *Meas. Sci. Technol.*, *1*, 592–595.

Hartogh, P., and Ch. Jarchow (1995), Ground-based detection of middle atmospheric water vapour, global process monitoring and remote sensing of the ocean and sea ice, edited by D. W. Deering and P. Gudmandsen, *Proc. SPIE*, Vol. 2586, 188–195.

Hartogh, P., G. K. Hartmann, and P. Zimmermann (1991), Simultaneous water vapor and ozone measurements with millimeter-waves in the strato-

sphere and mesosphere, *IEEE Catalog Number 91CH2971-0*, *1*, 227–230.
Hartogh, P., Ch. Jarchow, G. R. Sonnemann, and M. Grygalashvyly (2004), On the spatiotemporal behavior of ozone within the upper mesosphere/mesopause region under nearly polar night conditions, *J. Geophys. Res.*, *109*, D18303, doi:10.1029/2004JD004576.
Hirota, I., and T. Hirooka (1984), Normal mode Rossby waves observed in the upper stratosphere. Part I: First symmetric modes of zonal wavenumbers 1 and 2, *J. Atmos. Sci.*, *41*, 1253–1267.
Hirota, I., Y. Maekawa, S. Fukao, K. Fukuyama, M. P. Sulzer, J. L. Fellous, T. Tsuda, and S. Kato (1983), Fifteen-day observation of mesospheric and lower thermospheric motions with the aid of the Arecibo UHF radar, *J. Geophys. Res.*, *88*, 6835–6842.
Julian, P. R. (1971), Some aspects of variance spectra of synoptic scale tropospheric wind components in midlatitudes and in the tropics, *Mon Weather Rev.*, *99*, 954–965.
Kirkwood, S., and A. Réchou (1998), Planetary wave modulation of PMSE, *Geophys. Res. Lett.*, *25*, 4509–4512.
Kirkwood, S., V. Barabash, U. E. Brändström, A. Möstrom, and K. Stebel (2002), Noctilucent clouds, PMSE and 5-day planetary waves: A case study, *Geophys. Res. Lett.*, *29*(10), 1411, doi:10.1029/2001GL014022.
Körner, U., and G. R. Sonnemann (2001), Global three-dimensional modelling of the water vapour concentration of the mesosphere-mesopause region and implications with respect to the noctilucent cloud region, *J. Geophys. Res.*, *106*, 9639–9651.
Liu, H.-L., E. R. Talaat, G. R. Roble, R. S. Lieberman, D. M. Riggin, and J.-H. Yee (2004), The 6.5-day wave and its seasonal variability in the middle and upper atmosphere, *J. Geophys. Res.*, *109*, D21112, doi:10.1029/2004JD004795.
Lübken, F.-J. (1997), Seasonal variation of turbulent energy dissipation rates at high latitudes as determined by in situ measurements of neutral density fluctuations, *J. Geophys. Res.*, *102*, 13,441–13,445.
Lübken, F.-J., A. Müllemann, and M. A. Jarvis (2004), Temperature and horizontal winds in the Antarctic summer mesosphere, *J. Geophys. Res.*, *109*, D24112, doi:10.1029/2004JD005133.
Madden, R. A. (1978), Further evidence of traveling planetary waves, *J. Atmos. Sci.*, *35*, 1605–1618.
Madden, R. A. (1979), Observation of large-scale traveling Rossby waves, *Rev. Geophys. Space Phys.*, *17*, 1935–1949.
Manson, A. H., C. E. Meek, J. B. Gregory, and D. K. Chakrabarty (1982), Fluctuations in tidal (24-, 12-h) characteristics and oscillations (8-h–5-d) in the mesosphere and lower thermosphere (70–110 km); Saskatoon (52°N, 107°W), 1979–1981, *Planet. Space Sci.*, *30*, 1283–1294.
Massebeuf, M., R. Bernard, J. L. Fellous, and M. Glass (1981), Simultaneous meteor radar observations at Monpazier (France, 44°N) and Punta Borinquen (Puerto Rico, 18°N), *J. Atmos. Terr. Phys.*, *43*, 535–542.
Merkel, A. W., G. E. Thomas, S. E. Palo, and S. M. Bailey (2003), Observations of the 5-day planetary wave in PMC measurements from the Student Nitric Oxide Explorer, *Geophys. Res. Lett.*, *30*(4), 1196, doi:10.1029/2002GL016524.
Meyer, C. K., and J. M. Forbes (1997), A 6.5-day westward propagating planetary wave: Origin and characteristics, *J. Geophys. Res.*, *102*, 26,173–26,178.
Miyoshi, Y. (1999), Numerical simulation of the 5-day and 16-day waves in the mesopause region, *Earth Planets Space*, *51*, 763–772.
Riggin, D. M., et al. (2006), Observations of the 5-day wave in the mesosphere and lower thermosphere, *J. Atmos. Sol. Terr. Phys.*, *68*, 323–339.
Rodgers, C. D. (1976), Evidence for the five-day wave in the upper stratosphere, *J. Atmos. Sci.*, *33*, 710–711.
Rosenlof, K. H., and R. J. Thomas (1990), Five-day mesospheric waves observed in Solar Mesosphere Explorer ozone, *J. Geophys. Res.*, *95*(D4), 895–899.
Salby, M. L. (1981), Rossby normal modes in nonuniform background configurations. Part II: Equinox and solstice conditions, *J. Atmos. Sci.*, *38*, 1247–1254.
Salby, M. L. (1984), Survey of planetary-scale traveling waves: The state of theory and observations, *Rev. Geophys. Space Phys.*, *22*, 209–236.
Seele, C., and P. Hartogh (1999), Water vapour of the polar middle atmosphere: Annual variation and summer mesosphere conditions as observed by ground-based microwave spectroscopy, *Geophys. Res. Lett.*, *26*, 1517–1520.
Shimazaki, T. (1985), Minor Constituents in the Middle Atmosphere, D. Reidel, Norwell, Mass.
Sonnemann, G. R. (2001), The photochemical effects of dynamically induced variations in solar insolation, *J. Atmos. Sol. Terr. Phys.*, *63*, 781–797.
Sonnemann, G. R., and M. Grygalashvyly (2003), The zonal wind effect on the photochemistry within the mesosphere/mesopause region, *Adv. Space Res.*, *32*(5), 719–724.
Sonnemann, G. R., and M. Grygalashvyly (2005a), Solar influence on mesospheric water vapor with impact on NLCs, *J. Atmos. Sol. Terr. Phys.*, *67*, 177–190.
Sonnemann, G. R., and M. Grygalashvyly (2005b), On the two-day oscillation and the day-to-day variability in global 3-D-modeling of the chemical system of the upper mesosphere/mesopause region, *Nonlin. Proc. Geophys.*, *12*, 691–705.
Sonnemann, G. R., M. Grygalashvyly, and U. Berger (2005), Autocatalytic water vapor production as a source of large mixing ratios within the middle to upper mesosphere, *J. Geophys. Res.*, *110*, D15303, doi:10.1029/2004JD005593.
Sonnemann, G. R., M. Grygalashvyly, and U. Berger (2006), Impact of stratospheric warming event in January 2001 on the minor constituents in the MLT region calculated on the basis of a new 3D-model LIMA of the dynamics and chemistry of the middle atmosphere, *J. Atmos. Sol. Terr. Phys.*, *68*, 2012–2025.
Sonnemann, G. R., P. Hartogh, Ch. Jarchow, M. Grygalashvyly, and U. Berger (2007), On the winter anomaly of the night-to-day ratio of ozone in the middle to upper mesosphere in middle to high latitudes, *J. Adv. Space Res.*, in press.
Sugiyama, T., Y. Murako, H. Sogawa, and S. Fukao (1996), Oscillations in polar mesospheric summer echoes and bifurcation of noctilucent cloud formation, *Geophys. Res. Lett.*, *23*, 653–656.
Uppala, S. M., et al. (2005), The ERA-40 re-analysis, *Q. J. R. Meteorol. Soc.*, *131*, 2961–3012.
Venne, D. E. (1985), The horizontal structure of traveling planetary scale-waves in the upper stratosphere, *J. Geophys. Res.*, *90*, 3869–3879.
Venne, D. E. (1989), Normal-mode Rossby waves observed in the wavenumber 1–5 geopotential fields of the stratosphere and troposphere, *J. Atmos. Sci.*, *46*, 1042–1056.
Vincent, R. A. (1984), MF/HF radar measurements of the dynamics of the mesopause region-A review, *J. Atmos. Terr. Phys.*, *46*, 961–974.
von Savigny, C., H. Bovensmann, J. P. Burrows, M. J. Schwartz, and D. L. Wu (2006), Noctilucent cloud studies with Envisat/SCIAMACHY: Observations of the 5-day wave, Contribution to 36th COSPAR Scientific Assembly, Beijing, China, July 16–23.
Walcek, C. J. (2000), Minor flux adjustment near mixing ratio extremes for simplified yet highly accurate monotonic calculation of tracer advection, *J. Geophys. Res.*, *105*, 9335–9348.
Wallace, J. M., and C.-P. Chang (1969), Spectrum analysis of large scale disturbances in the tropical lower troposphere, *J. Atmos. Sci.*, *26*, 1010–1025.
Williams, C. R., and S. K. Avery (1992), Analysis of long-period waves using the mesosphere-stratosphere-troposphere radar at Poker Flat, Alaska, *J. Geophys. Res.*, *97*, 20,855–20,861.
Woods, T. N., W. K. Tobiska, G. J. Rottman, and J. R. Worden (2000), Improved solar Lyman irradiance modeling from 1947 through 1999 based on UARS observations, *J. Geophys. Res.*, *105*, 27,195–27,215.
Wu, D. L., P. B. Hays, and W. R. Skinner (1994), Observations of the 5-day wave in the mesosphere and lower thermosphere, *Geophys. Res. Lett.*, *21*(24), 2733–2736.

U. Berger, M. Grygalashvyly, and G. R. Sonnemann, Leibniz-Institute of Atmospheric Physics at the University Rostock in Kühlungsborn, Schloss-Str.6, D-18225 Ostseebad Kühlungsborn, Germany. (gryga@ap-kborn.de)
P. Hartogh and S. Li, Max-Planck-Institute for Solar System Research, Max-Planck-Str. 2, D-37191 Katlenburg-Lindau, Germany.